ELSEVIER

International Journal of Mass Spectrometry 210/211 (2001) 1–11

International Journal of Mass Spectrometry

www.elsevier.com/locate/ijms

A high-level ab initio investigation of identity and nonidentity gas-phase S_N2 reactions of halide ions with halophosphines

Theis I. Sølling[a,1], Addy Pross[b], Leo Radom[a,*]

[a]*Research School of Chemistry, Australian National University, Canberra, ACT 0200, Australia*
[b]*Department of Chemistry, Ben Gurion University of the Negev, Beer Sheva, Israel*

Received 8 December 2000; accepted 16 February 2001

Abstract

The high-level ab initio procedures G2(+) and G2(+)[ECP(S)]have been employed in an investigation of S_N2 reactions at neutral tri-coordinated phosphorus. The process has been modeled by identity and nonidentity substitution reactions involving a series of halophosphines PH_2–X and halide ions. We find that the reaction proceeds without an intervening barrier by way of a tetra-coordinated phosphorus anion intermediate ($X–PH_2–Y^-$). This contrasts with the corresponding process for the carbon and nitrogen analogues, where the tetra-coordinated species is a transition structure. The threshold for inversion of the phosphorus intermediate is found to lie below the reaction energy in the cases where F^- is the leaving group, but above it in all the other cases. The S_N2 reaction will therefore lead to racemization when F^- is expelled. In the other cases, it is possible in principle that the reaction can be controlled to proceed with inversion, but because of the relatively low barriers for inversion, this is not a very likely outcome. We predict that the tetra-coordinated intermediate should be detectable, if not isolable, and that the S_N2 reaction at neutral tri-coordinated phosphorus is exothermic when the reactant halide ion is more electronegative than the product halide ion, and endothermic when the reverse applies. (Int J Mass Spectrom 210/211 (2001) 1–11) © 2001 Elsevier Science B.V.

Keywords: Nucleophilic substitution; Halophosphines; G2; ECP; Pseudorotation

1. Introduction

The S_N2 reaction of saturated alkyl halides with halide ions is prominent in organic chemistry. In recent years it has been the subject of a considerable number of experimental [1] and theoretical studies [2,3], and its mechanism is therefore well established. It is, for example generally accepted that the lowest-energy pathway of S_N2 reactions in the gas phase follows a double-well potential and involves the well-known inversion transition structure [4]. In a computational study of S_N2 reactions at neutral nitrogen, we found a similar pattern of behavior [5]. This result is in line with several experimental investigations [6] and earlier theoretical [7] studies.

In contrast to these intensively studied reactions at saturated carbon and nitrogen, mechanistic studies of

* Corresponding author. E-mail address: radom@rsc.anu.edu.au

[1] Present address: Arthur Amos Noyes Chemical Physics Laboratory, California Institute of Technology, Pasadena, California 91125, USA

Dedicated to Professor Nico Nibbering on the occasion of his formal retirement from the University of Amsterdam and in recognition of his outstanding contributions to gas-phase ion chemistry.

PII S1387-3806(01)00426-2

S_N2 reactions at neutral tri-coordinated phosphorus, i.e.

$$Y^- + PH_2{-}X \rightarrow Y{-}PH_2 + X^- \quad (1)$$

are scarce [8–11] and inconclusive. For example, the question of whether such S_N2 reactions proceed in a concerted or a stepwise manner remains open. In addition, the stereochemistry of the reaction is unclear, given that the entire span of stereochemical outcomes ranging from inversion to retention of configuration have been observed [8–10,12,13].

In an attempt to shed light on this opaque corner of nucleophilic substitution reactions, we have embarked on a systematic high-level ab initio investigation of the S_N2 reactions involving halophosphines (PH_2–X) and halide ions (Y^-) (X,Y = F, Cl, Br, I).

2. Computational methods

Ab initio molecular orbital calculations [14] were carried out using modified forms of G2 theory [15] with the GAUSSIAN 94 [16] and GAUSSIAN 98 [17] program packages. The modifications have been introduced to allow for a better description of anions, and to reduce the computational cost, primarily in the calculations involving bromine- and iodine-containing species. First, to obtain a better description of anions, we have substituted the standard 6-31G(*d*) basis set in the geometry optimization by the 6-31+G(*d*) basis set. Second, to reduce the computational cost, the frozen-core approximation was employed in the geometry optimization, and Stuttgart energy-adjusted effective core potentials (ECPs) and valence basis sets [18] were used for bromine- and iodine-containing species. In geometry optimizations of such species, a [31,31] contraction scheme was used, whereas single-point calculations employ the uncontracted (4*s*,4*p*)→[1111,1111] sets. These basis sets were augmented with the appropriate number of *s* and *p* diffuse functions as well as with *p*, *d*, and *f* polarization functions. For the splitting of the *d* functions, nongeometrical splittings were employed as recommended previously [19,20]. These procedures result in two modified G2 methods, which have previously been referred to as G2(+) and G2(+)[ECP(S)] [5]. They have been shown to yield reliable thermochemical quantities [3,19]. In addition, the standard HF/6-31+G(*d*) ZPVEs have been substituted in the present work by MP2(fc)/6-31+G(*d*) ZPVEs scaled by 0.9670 [21] because of certain inconsistencies between the two levels [22]. However, for convenience we shall still refer to these levels of theory as G2(+) and G2(+)[ECP(S)]. Table 1 presents the G2(+) and G2(+)[ECP(S)] total energies of the species investigated. Relative energies within the text correspond to G2(+) values at 0 K for fluorine- and chlorine-containing species and to G2(+)[ECP(S)] values at 0 K for bromine- and iodine-containing species.

Table 1
G2(+)[a] and G2(+)[ECP(S)][b] total energies (Hartrees, 0 K)

Species	Energy	Species	Energy
F^-	−99.760 60	**15**	−901.645 73
Cl^-	−459.809 00	**16**	−455.257 38
Br^-	−13.429 88	**17**	−541.657 24
I^-	−11.460 56	**18**	−541.654 61
1	−441.856 50	**TS: 6 → 15**	−901.636 30
2	−801.846 77	**TS: 15 → 6***	−901.643 92
3	−355.456 94	**TS: 7 → 16**	−455.249 78
4	−353.476 69	**TS: 16 → 7***	−455.257 33
5	−541.685 25	**TS: 5 → 17**	−541.646 30
6	−901.695 02	**TS: 17 → 18**	−541.637 93
7	−455.311 25	**TS: 18 → 18′**	−541.647 61
8	−453.337 14	**TS: 8 → 8***	−453.273 26
9	−1261.695 04	**TS: 9 → 9***	−1261.639 91
10	−815.309 35	**TS: 10 → 10***	−815.253 80
11	−813.332 85	**TS: 11 → 11***	−813.276 69
12	−368.923 51	**TS: 12 → 12***	−368.867 82
13	−366.946 86	**TS: 13 → 13***	−366.890 90
14	−364.969 98	**TS: 14 → 14***	−364.913 99

[a] Fluorine- and chlorine-containing molecules.
[b] Bromine- and iodine-containing molecules.

3. Results and discussion

The potential energy surfaces for the lowest-energy pathway of the gas-phase S_N2 reactions of a monohalophosphine (PH_2–X) and halide ion (Y^-), for different combinations of halophosphine and halide ion, all have a similar form. The halophosphine combines with the anion in a barrier-free exothermic

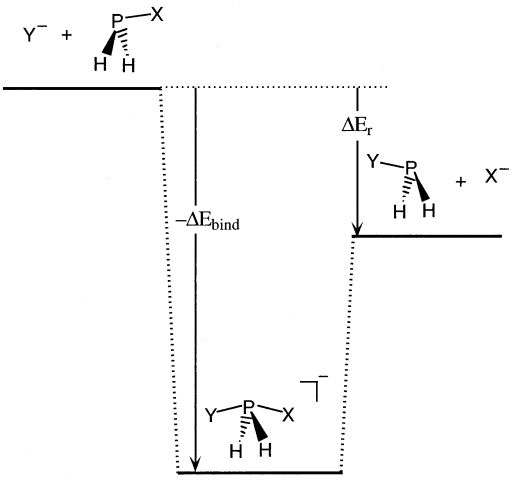

Fig. 1. Generalized energy profile for the $Y^- + PH_2 - X \rightarrow Y - PH_2 + X^-$ S_N2 reactions. X and Y are chosen among F, Cl, Br, or I.

process to form an intermediate tetra-coordinated phosphorus species $[Y–PH_2–X]^-$. This species then dissociates to the product halophosphine ($Y–PH_2$) and halide anion (X^-) in an endothermic step which, in the reverse direction, is also barrier-free. Thus, there are no transition structures along the reaction coordinate for the S_N2 reactions of monohalophosphines with halide ions. This reactivity pattern is depicted schematically in Fig. 1. The MP2(fc)/6-31G+(*d*) optimized structures and selected geometrical parameters of the halophosphines are shown in Fig. 2, whereas Fig. 3 displays the optimized geometries of the intermediate tetra-coordinated phosphorus species.

In the following sections, the energetics of the set

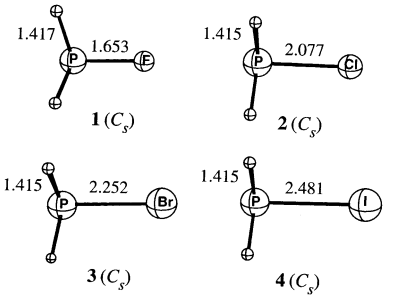

Fig. 2. Optimized (MP2(fc)/6-31+G(*d*)) geometries of the halophosphines PH_2–X. Bond lengths are in units of angstroms.

of S_N2 reactions are discussed in detail. Also, the feasibility and stereochemistry of such reactions are examined. For both sets of results, comparisons are made with the results of our previous investigations of the corresponding nitrogen and carbon systems [3,5].

3.1. Reaction energies

The reaction energies, ranging up to 209.4 kJ-mol^{-1} in magnitude, are presented in Table 2. The data show that the reactions of a specific halophosphine with varying halide ions (Y^-) become increasingly endothermic (or less exothermic) in the order: $F^- < Cl^- < Br^- < I^-$. Conversely, the reactions of a specific halide ion with varying halophosphines become more exothermic in the order: $PH_2–F < PH_2–Cl < PH_2–Br < PH_2–I$. These two observations are of course coupled and can be rationalized in terms of a simple thermodynamic cycle (Scheme 1).

$$
\begin{array}{lcccccl}
Y^- & & & \longrightarrow & Y^{\bullet} & + & e^- \quad EA(Y) \\
X^{\bullet} & + & e^- & \longrightarrow & & & X^- \quad -EA(X) \\
 & & PH_2–X & \longrightarrow & PH_2^{\bullet} & + & X^{\bullet} \quad E_{dissoc}(P–X) \\
Y^{\bullet} & + & PH_2^{\bullet} & \longrightarrow & Y–PH_2 & & -E_{dissoc}(P–Y) \\
\hline
Y^- & + & PH_2–X & \longrightarrow & Y–PH_2 & + & X^- \quad \Delta E_r
\end{array}
$$

$$\Delta E_r = EA(Y) - EA(X) + E_{dissoc}(P–X) - E_{dissoc}(P–Y)$$

Scheme 1

It can be seen that the reaction energy is just the sum of two energetic contributions: the difference between the electron affinities of $Y^{\bullet}$ and $X^{\bullet}$, and the difference between the P–X and P–Y bond energies. Given that the electron affinities of $F^{\bullet}$, $Cl^{\bullet}$, $Br^{\bullet}$, and $I^{\bullet}$ lie in a relatively narrow range (Table 3) [23], whereas bond strengths to halogens typically vary significantly, decreasing from F to I (see, e.g. Table 3) [24], this indicates that the reaction energies are dominated by the relative strengths of the different phosphorus–halogen bonds. Thus, the S_N2 reaction is exothermic whenever the less electronegative halide is displaced (Table 2). The exothermicity is particularly pronounced when the incoming halogen (Y^-) is F^-, which may be attributed to the high P–F bond

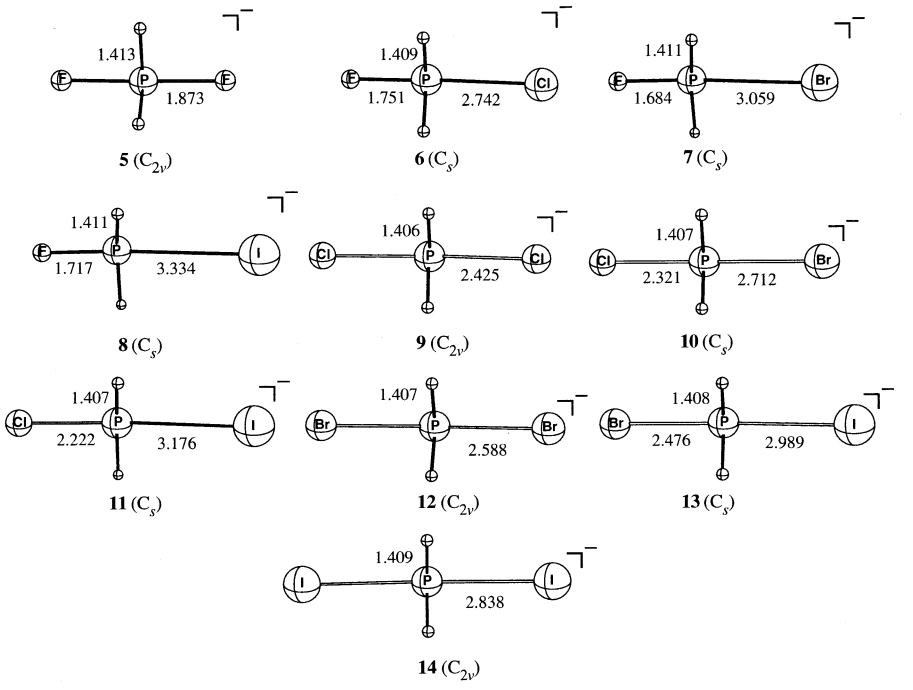

Fig. 3. Optimized (MP2/6-31+G(*d*)) geometries of the tetra-coordinated phosphorus intermediates Y–PH_2–X–involved in the S_N2 reactions at tri-coordinated phosphorus. Bond lengths are in units of angstroms.

strength (Table 3). Further evidence in this direction can be obtained from a comparison with the reaction energies in the corresponding carbon and nitrogen cases (see Sec. 3.6).

3.2. Binding energies of the tetra-coordinated phosphorus species

The binding energies of the intermediate tetra-coordinated phosphorus adducts between a halide ion and a halophosphine to form $[Y–PH_2–X]^-$, calculated relative to $Y^-+PH_2–X$, are included in Table 2. Calculated values range between 52.7 and 262.2 kJ mol^{-1}. The magnitudes of the binding energies increase with increasing electronegativity of Y but decrease with increasing electronegativity of X. Binding energies of $[Y–PH_2–X]^-$, when calculated with respect to the lower-energy dissociation products (either $Y^-+PH_2–X$ or $Y–PH_2+X^-$), tend to be greatest in the symmetrical cases (X=Y) and to decrease in the order F>Cl>Br>I. The changes in binding energy with variation in Y may be attributed to reduced P–Y bonding as the size of the halide ion Y^- increases, This trend is in line with data for the proton-bound dimers of halide ions, as discussed previously by Shaik and Shurki [25].

3.3. Feasibility of S_N2 reactions at tri-coordinated phosphorus

Since the S_N2 reactions at tri-coordinated phosphorus do not have any intermediate barrier, their feasibility as gas-phase reactions will be solely governed by the reaction energy. Accordingly, a clear prediction may be made for the formation of fluorophosphine from chloro-, bromo-, or iodophosphine since these reactions are accompanied by a substantial exothermicity (Table 2). Thus, it would seem that S_N2 reactions involving a reactant fluoride ion and a halophosphine should, indeed, be feasible. Conversely, the endothermicity of the reaction between any halide ion (other than F^-) and PH_2F is consider-

Table 2
Reaction energies (ΔE_r) for S_N2 reactions involving halophosphines ($PH_2 - X$) and halide ions (Y^-), and binding energies (ΔE_{bind}) of the associated tetra-coordinated phosphorus species ($Y - PH_2 - X^-$)[a]

Halophosphine ($PH_2 - X$)		Ion (Y^-)	ΔE^b_{bind}	ΔE^b_r
$PH_2 - F$	**1**	F^-	178.9	0.0
		Cl^-	77.5	152.6
		Br^-	65.3	180.7
		I^-	52.7	209.4
$PH_2 - Cl$	**2**	F^-	230.1	−152.6
		Cl^-	103.1	0.0
		Br^-	85.9	28.1
		I^-	67.0	56.8
$PH_2 - Br$	**3**	F^-	246.0	−180.7
		Cl^-	114.0	−28.1
		Br^-	96.3	0.0
		I^-	77.1	28.7
$PH_2 - I$	**4**	F^-	262.2	−209.4
		Cl^-	123.8	−56.8
		Br^-	105.8	−28.7
		I^-	85.9	0.0

[a] G2(+) or G2(+)[ECP(S)] values in kJ/mol^{-1} at 0 K.
[b] Calculated relative to Y^- plus PH_2− X, see Fig. 1.

able, and therefore such reactions would be unlikely to take place. More generally, it would appear that a nonidentity reaction between a halophosphine and a halide ion is likely to be successful when the reactant halide ion is more electronegative than the product halide ion. Identity reactions, being thermoneutral, should also be feasible.

3.4. Existence of the tetra-coordinated phosphorus species

The combination of a halide ion and a halophosphine to form a tetra-coordinated phosphorus species is accompanied in most cases by a significant binding energy. Thus, quite apart from being involved in the reaction mechanism for S_N2 at tri-coordinated phosphorus, the intermediate is of interest in its own right. Accordingly, we predict that adducts of this type should be experimentally observable under appropriate conditions. The most stable intermediates correspond to the symmetrical cases ($[X–PH_2–X]^-$).

Table 3
Experimental electron affinities (EAs) of halogen radicals and calculated homolytic dissociation energies (E_{dissoc}) of halophosphines[a]

Halogen radical	EA[b]	Halophosphine	E^c_{dissoc}
F·	3.401 (3.477)	$PH_2 - F$	4.763
Cl·	3.601 (3.602)	$PH_2 - Cl$	3.306
Br·	3.364 (3.297)	$PH_2 - Br$	2.710
I·	3.059 (2.958)	$PH_2 - I$	2.074

[a] Values in eV, experimental data are taken from [23]. 1 eV = 96.485 kJ/mol^{-1}.
[b] Numbers in parentheses are calculated G2(+) or G2(+)[ECP(S)] values (0 K).
[c] G2(+) or G2(+)[ECP(S)] values (0 K).

3.5. Stereochemistry of the S_N2 reaction at tri-coordinated phosphorus

Tri-coordinated phosphorus compounds generally have high inversion barriers and it is therefore possible to obtain optically pure phosphines [26]. The intermediate in an S_N2 reaction which involves a chiral phosphine is also chiral, as can be seen in

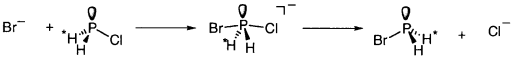

(2)

Consequently, the reaction should be stereospecific [27]. However, because the intermediate can in principle undergo an inversion of configuration, then the size of the inversion barrier will determine the actual stereoselectivity of the reaction [28]. A high barrier for the inversion of the intermediate would effectively preclude this process and a high degree of stereoselectivity should result. If, on the other hand, the barrier for the inversion of the intermediate is low, the stereochemical integrity of the phosphorus center may be lost and the product halophosphine would be expected to be racemic. Mechanisms including Berry pseudorotation or "turnstile" rotation of the type depicted in Fig. 4, have been suggested for penta-coordinated phosphorus compounds [28–30]. It has been found that pseudorotation is dominant in the apical/equatorial ligand interchange of symmetric penta-coordinated phosphorus species (e.g. PH_5) [28]. However, the processes that bring about ligand inter-

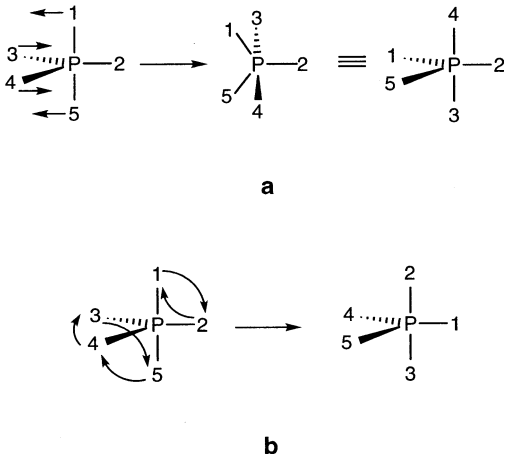

Fig. 4. Two mechanistic proposals for interchange of ligands in PX_5: (a) Berry pseudorotation ([29]), and (b) "turnstile" rotation ([30]).

change in unsymmetric phosphoranes (e.g. PH_3F_2) and in systems with a lone-pair acting as a phantom ligand are much more complicated [28,31]. Our results for the ligand interchanges that lead to inversion in the $[X–PH_2–Y]^-$ intermediates are in line with these findings.

We initially investigated the possibility of direct inversion by way of a planar transition structure for the identity reactions. However, we find that such planar species lie high in energy (e.g., planar $[Br–PH_2–Br]^-$ lies at 116.3 kJ mol^{-1} relative to the separated products, i.e. at 212.7 kJ mol^{-1} relative to the tetra-coordinated intermediate) and, in the cases of $F–PH_2–F^-$and $Cl–PH_2–Cl^-$, represent higher-order saddle points.

Fig. 5 displays the lowest energy pathway for the inversion process in

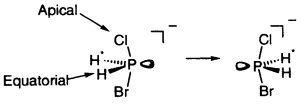

(3)

A pathway of this type involving a single transition structure is followed in most of the cases investigated (Table 4). The geometries of the transition structures for inversion are presented in Fig. 6. The inversion

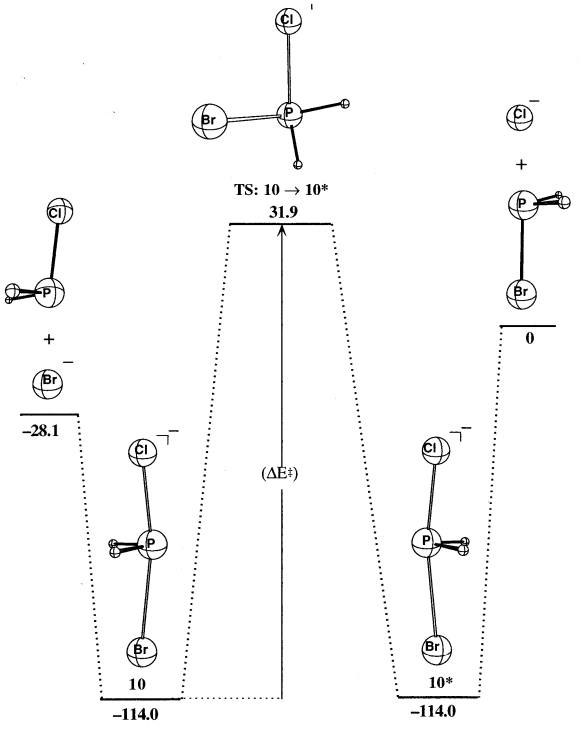

Fig. 5. Schematic representation of the potential energy surface for the one-step inversion of the tetra-coordinated intermediates in the Br^-+PH_2Cl S_N2 reaction. All energies (kJ mol^{-1}) are given relative to PH_2Br+Cl^-.

barriers are generally about 145–147 kJ mol^{-1} but there is a somewhat higher barrier of 167.7 kJ mol^{-1} for $F–PH_2–I^-$.

The lowest-energy pathway for inversion of $F–PH_2–Cl^-$ is shown in Fig. 7. It can be seen that the inversion proceeds by way of an additional confor-

Table 4
Barriers for the one-step inversion processes[a]

Intermediate		$\Delta E‡$ [b]
$F-PH_2-I^-$	**8**	167.7
$Cl-PH_2-Cl^-$	**9**	144.8
$Cl-PH_2-Br^-$	**10**	145.9
$Cl-PH_2-I^-$	**11**	147.4
$Br-PH_2-Br^-$	**12**	146.2
$Br-PH_2-I^-$	**13**	146.9
$I-PH_2-I^-$	**14**	147.0

[a] G2(+) or G2(+)[ECP(S)] values in kJ mol^{-1} at 0 K.
[b] Inversion barriers calculated relative to the tetra-coordinated intermediate: see Fig. 5.

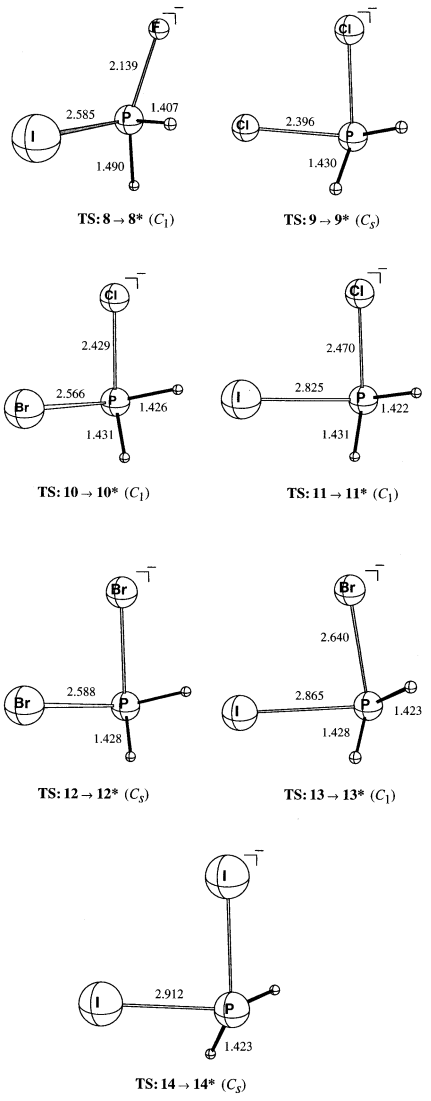

Fig. 6. Optimized MP2(fc)/6-31+G(*d*) geometries of the species involved in the one-step inversion of the tetra-coordinated intermediates. Bond lengths are in units of angstroms.

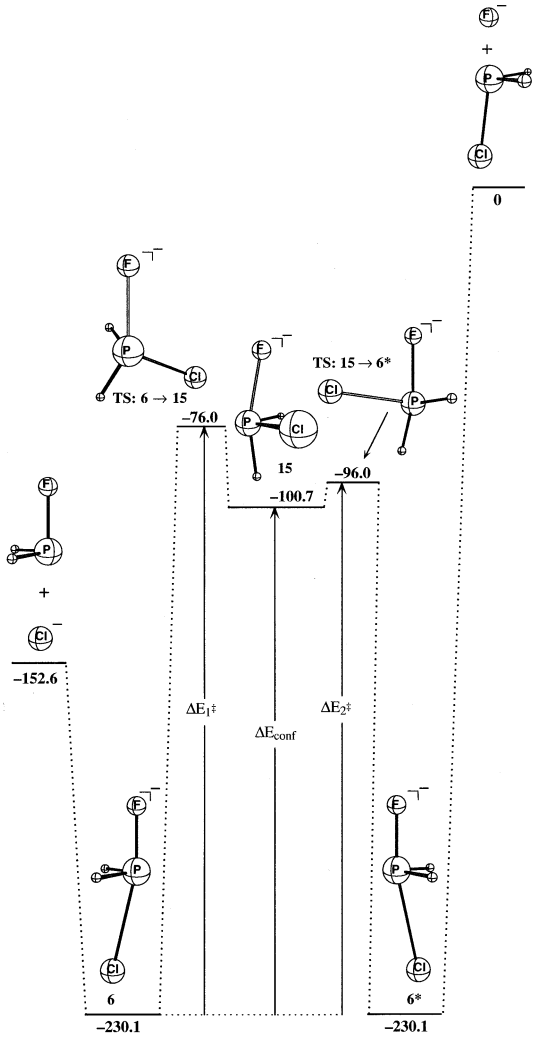

Fig. 7. Schematic representation of the potential energy surface for the two-step inversion of the tetra-coordinated intermediates in the $Cl^- + PH_2F$ S_N2 reaction. All energies (kJ mol^{-1}) are given relative to $PH_2Cl + F^-$.

mation of the intermediate tetra-coordinated phosphorus species, having one apical and one equatorial halide substituent, and therefore involves two transition structures. The lowest-energy pathway for the inversion of $F–PH_2–Br^-$ has a similar form. The relevant thermochemical data for these two systems are listed in Table 5 and the optimized geometries of the species involved are presented in Fig. 8. For $F–PH_2–Br^-$ and $F–PH_2–Cl^-$, structures with the fluorine substituent in an equatorial position do not correspond to minima.

The inversion of $F–PH_2–F^-$ is even more complicated than that of $F–PH_2–Cl^-$. The potential energy surface for the process is symmetric around the transition structure (**TS: 18 → 18′**) which connects the two possible isomers with one apical and one equatorial fluorine substituent. Apparently the high electronegativity of fluorine and the high proton

Table 5
Barriers for the two-step inversion process and energies for the higher-energy conformer[a]

Inverting molecule		$\Delta E_1^{\ddagger}$ [b]	ΔE_{conf}^{b}	$\Delta E_2^{\ddagger}$ [b]
$F-PH_2-Cl^-$	6	154.1	129.4	134.1
$F-PH_2-Br^-$	7	161.4	141.4	141.6

[a] G2(+) or G2(+)[ECP(S)] values in kJ mol^{-1} at 0 K, calculated relative to the more stable conformer of the tetra-coordinated intermediate.
[b] See Fig. 7.

affinity of F^- result in the formation of an intermediate complex (**17**) between HF and HPF^- en route to **18** (Fig. 9). The detailed geometric features of the intermediates and transition structures are shown in Fig. 10. It is worth noting that the inversion of $F–PH_2–F^-$ involves two conformers with one apical and one axial halogen substituent (connected by **TS: 18 → 18′**) as opposed to the inversion of $F–PH_2–Cl^-$ which involves only one such conformer. Again, this arises because species with one equatorial and one apical halogen substituent do not appear to correspond to minima unless fluorine is in the apical position.

For all the S_N2 reactions where fluoride ion is expelled, the transition structures for inversion of the intermediate lie lower in energy than the product, and therefore it would be impossible for the tetra-coordinated intermediates to retain their configurational integrity during the course of the reaction. Accordingly, this type of substitution reaction should lead to a racemic halophosphine product. On the other hand, when Cl^-, Br^-, or I^- is expelled, the transition structure for inversion lies slightly higher in energy than the product, and in theory it might therefore be possible for the configuration of the intermediate to be retained under controlled conditions, thereby leading to an inverted product. These general predictions regarding the stereochemistry of gas-phase S_N2 reactions at tri-coordinated phosphorus will of course depend on the additional effect of the substituents that are required to create chirality. However, they are in line with the conclusions reached by Kyba [12] and by Pabel et al. [10] on the basis of experimental data. Kyba found that tetra-alkyl-coordinated phosphorus anions do not racemize easily, whereas Pabel et al. found that optically pure datively bonded fluorophosphines do indeed racemize.

It does not seem a simple matter to extend the above predictions beyond the reactions of halides and halophosphines. On the basis of the present results, we are not surprised by the broad range of stereochemical outcomes reported by Nielsen and Dahl [9] for condensed-phase S_N2 reactions involving neutral bases and various tri-coordinated phosphorus species.

3.6. Comparisons with the carbon and nitrogen systems

The striking similarity between the trigonal-bipyramidal-type transition structure in S_N2 reactions at saturated nitrogen and carbon on the one hand, and the tetra-coordinated phosphorus intermediate on the other, is evident. However, the tetra-coordinated phosphorus species is a local minimum and not a transition structure. This major difference is presumably related to the well-known fact that molecules that contain second-row elements frequently do not obey the octet rule (e.g. PF_5 is a well-known compound, whereas the corresponding carbon and nitrogen species are unknown).

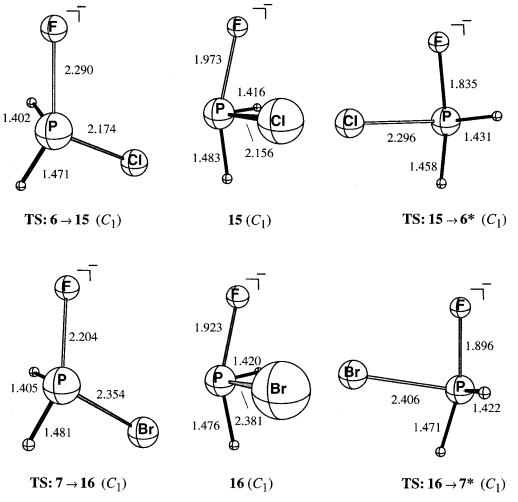

Fig. 8. Optimized MP2(fc)/6-31+G(*d*) geometries of the species involved in the two-step inversion of the tetra-coordinated intermediates $F–PH_2–Cl^-$ and $F–PH_2–Br^-$. Bond lengths are in units of angstroms.

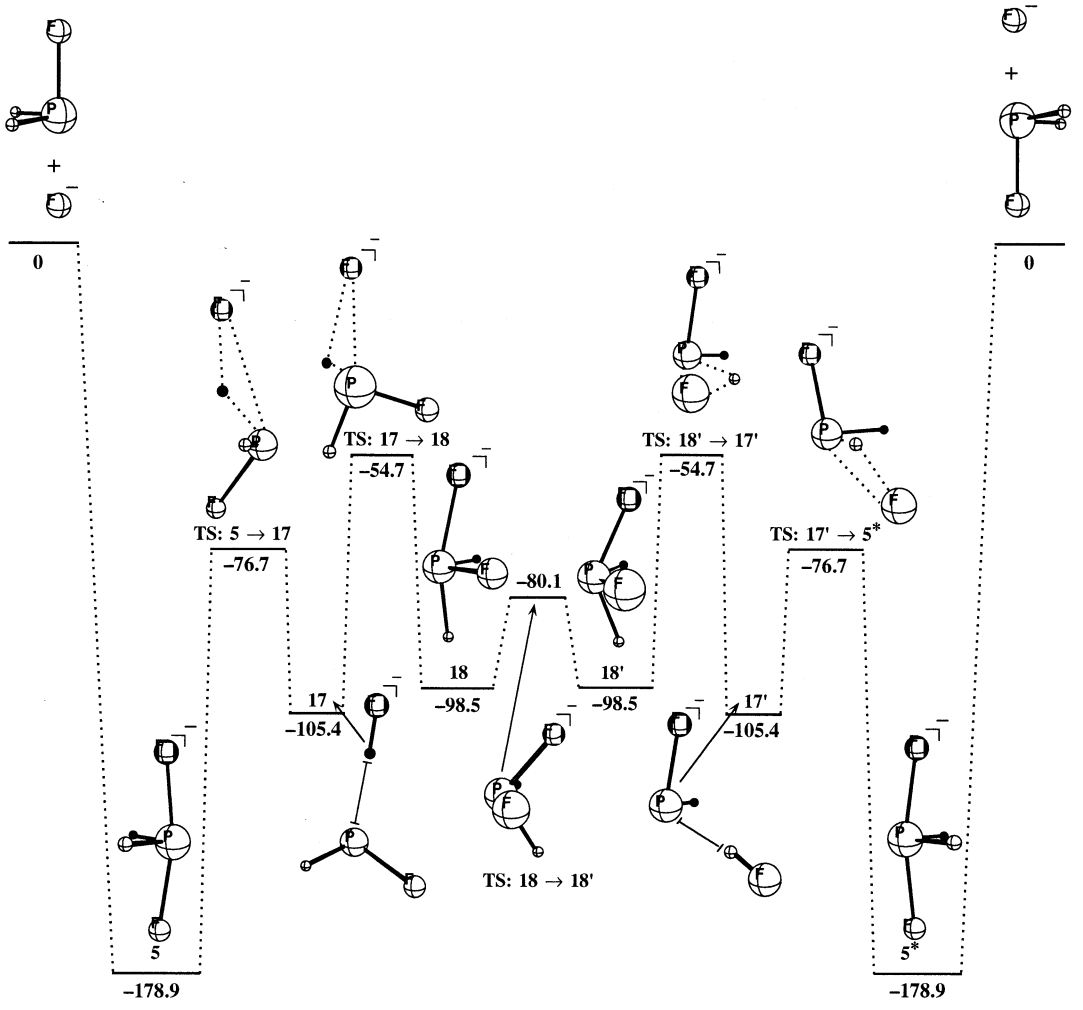

Fig. 9. Schematic representation of the potential energy surface for the inversion of F–PH_2–F^-. A single fluorine atom and a single hydrogen atom are shaded in order to simplify the visualization of the nuclear motion. All energies (kJ mol^{-1}) are given relative to PH_2F+F^-.

In general, we find that the energy changes for S_N2 reactions at carbon [3] and nitrogen [5] are similar to those of the corresponding reactions involving phosphorus. However, for S_N2 reactions of fluorophosphine, the reaction energies are significantly greater (–more endothermic by about 20–30 kJ mol^{-1}) than for the corresponding reactions involving fluoromethane or fluoramine. Equivalently, the reaction energies are more exothermic when a fluorophosphine is formed. This result is attributed to the greater strength of the P–F bond.

4. Concluding remarks

Gas-phase S_N2 reactions at tri-coordinated neutral monohalophosphines proceed in a barrier-free process by way of a tetra-coordinated anionic intermediate. This intermediate resembles the classical S_N2 transition structure. The intermediate tetra-coordinated species is generally strongly bound and should be observable in the gas phase. The S_N2 reaction itself should be feasible when the less electronegative halide ion is displaced because the reaction is exo-

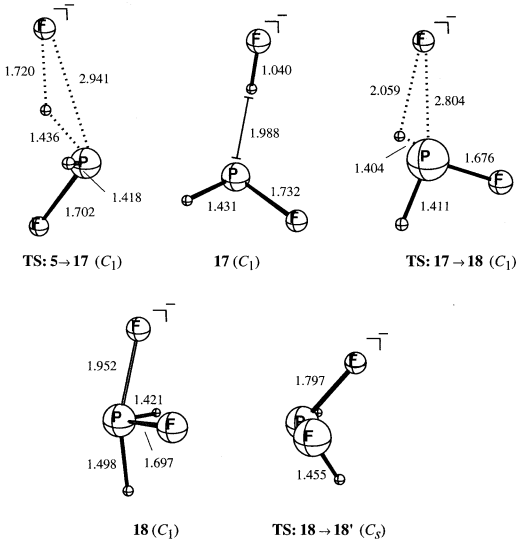

Fig. 10. Optimized MP2(fc)/6-31+G(*d*) geometries of the species involved in the inversion of F–PH_2–F^-. Bond lengths are in units of angstroms.

thermic in such instances. The reaction may in principle be controlled to proceed with inversion except when F^- is expelled, in which case it will lead to a racemic halophosphine product.

Acknowledgements

The authors thank Dr. Mikhail Glukhovtsev for his contributions during the initial stages of this project, Dr. Otto Dahl, University of Copenhagen for many helpful discussions, and they gratefully acknowledge generous allocations of time on the Fujitsu VPP-300 supercomputer and the SGI-Power Challenge of the Australian National University Supercomputer Facility.

References

[1] For recent gas-phase studies, see for example: J.M. Van Doren, C.H. DePuy, V. M. Bierbaum, J. Phys. Chem. 93 (1989) 1130; C.H. DePuy, S. Gronert, A. Mullin, V.M. Bierbaum, J. Am. Chem. Soc. 112 (1990) 8650; W.B. Knighton, J.A. Bognar, P.M. O'Connor, E. P. Grimsrud, ibid. 115 (1993) 12079; D.M. Cyr, G. Scarton, M.A. Johnson, J. Chem. Phys. 99 (1993) 4869; S.T. Graul, M.T. Bowers, J. Am. Chem. Soc. 116 (1994) 3875; C. Li, P. Ross, J.E. Szulejko, T.B. McMahon, ibid. 118 (1996) 9360.

[2] See for example: S.R. Van de Linde, W.L. Hase, J. Phys. Chem. 94 (1990) 2778; X.G. Zhao, S.C. Tucker, D.G. Truhlar, J. Am. Chem. Soc. 113 (1991) 826; S. Gronert, ibid. 113 (1991) 6041; S. Shaik, H.B. Schlegel, S. Wolfe, Theoretical Aspects of Organic Chemistry, The S_N2 Mechanism, Wiley, New York, 1992; I. Lee, C.K. Kim, D.S. Chung, B.-S. Lee, J. Org. Chem. 59 (1994) 4490; D.J. Mann, W.L. Hase, J. Phys. Chem. A 102 (1998) 6208.

[3] M.N. Glukhovtsev, A. Pross, L. Radom, J. Am. Chem. Soc. 117 (1995) 2024; 118 (1996) 6273.

[4] W.N. Olmstead, J.I. Brauman, J. Am. Chem. Soc. 99 (1977) 4219; M.J. Pellerite, J.I. Brauman, ibid. 102 (1980) 5993; M.J. Pellerite, J.I. Brauman, ibid. 105 (1983) 2672.

[5] M.N. Glukhovtsev, A. Pross, L. Radom, J. Am. Chem. Soc. 117 (1995) 9012.

[6] E. Erdik, M. Ay, Chem. Rev. 89 (1989) 1947; M. Novak, K.A. Martin, J.L. Heinrich, J. Org. Chem. 54 (1989) 5430; R. Ulbrich, M. Famulok, F. Bosold, G. Boche, Tetrahedron Lett. 31 (1990) 1689; P. Beak, J. Li, J. Am. Chem. Soc. 113 (1991) 2796.

[7] V.I. Minkin, B.Y. Simkin, R.M. Minyaev, Quantum Chemistry of Organic Compounds—Mechanisms of Reactions, Springer, Berlin, 1990, Chap. 5; M. Bühl, H.J. Schaefer, J. Am. Chem. Soc. 115 (1993) 364; M. Bühl, H.F. Schaefer, ibid. 115 (1993) 9143; R.M. Minyaev, D.J. Wales, J. Phys. Chem. 98 (1994) 7942.

[8] M. Mikolajczyk, Pure Appl. Chem. 52 (1980) 959; O. Dahl, Phosphorus and Sulfur 18 (1983) 201; O. Dahl, The Chemistry of Organophosphorus Compounds, F.R. Hartley (Ed.), Wiley, New York, 1996.

[9] J. Nielsen, O. Dahl, J. Chem. Soc. Perkin Trans. 2 (1984) 553.

[10] M. Pabel, A.C. Willis, S.B. Wild, Angew. Chem. Int. Ed. Engl. 33 (1994) 1835.

[11] J. Li, P. Beak, J. Am. Chem. Soc. 114 (1992) 9206.

[12] E.P. Kyba, J. Am. Chem. Soc. 98 (1976) 4805.

[13] C.R. Hall, T.C. Inch, Tetrahedron Lett. 17 (1976) 3645; G.S. Bajwa, W.G. Bentrude, ibid. 19 (1978) 421; G. Keglevich, L.D. Quin, Phosphorus Sulfur 26 (1986) 12.

[14] W.J. Hehre, L. Radom, P.v.R. Schleyer, J.A. Pople, Ab Initio Molecular Orbital Theory, Wiley, New York, 1986.

[15] L.A. Curtiss, K. Raghavachari, G.W. Trucks, J.A. Pople, J. Chem. Phys. 94 (1991) 7221.

[16] M.J. Frisch, G.W. Trucks, H.B. Schlegel, P.M.W. Gill, B.G. Johnson, M.A. Robb, J.R. Cheeseman, T. Keith, G.A. Petersson, J.A. Montgomery, K. Raghavachari, M.A. Al-Laham, V.G. Zakrzewski, J.V. Ortiz, J.B. Foresman, J. Cioslowski, B.B. Stefanov, A. Nanayakkara, M. Challacombe, C.Y. Peng, P.Y. Ayala, W. Chen, M.W. Wong, J.L. Andres, E.S. Replogle, R. Gomperts, R.L. Martin, D.J. Fox, J.S. Binkley, D.J. DeFrees, J. Baker, J.J.P. Stewart, M. Head-Gordon, C. Gonzalez, J.A. Pople, GAUSSIAN 94, Gaussian, Inc., Pittsburgh, PA, 1995.

[17] M.J. Frisch, G.W. Trucks, H.B. Schlegel, G.E. Scuseria, M.A. Robb, J.R. Cheeseman, V.G. Zakrzewski, J.A. Montgomery Jr., R.E. Stratmann, J.C. Burant, S. Dapprich, J.M. Millam,

A.D. Daniels, K.N. Kudin, M.C. Strain, O. Farkas, J. Tomasi, V. Barone, M. Cossi, R. Cammi, B. Mennucci, C. Pomelli, C. Adamo, S. Clifford, J. Ochterski, G.A. Petersson, P.Y. Ayala, Q. Cui, K. Morokuma, D.K. Malick, A.D. Rabuck, K. Raghavachari, J.B. Foresman, J. Cioslowski, J.V. Ortiz, B.B. Stefanov, G. Liu, A. Liashenko, P. Piskorz, I. Komaromi, R. Gomperts, R.L. Martin, D.J. Fox, T. Keith, M.A. Al-Laham, C.Y. Peng, A. Nanayakkara, C. Gonzalez, M. Challacombe, P.M.W. Gill, B. Johnson, W. Chen, M.W. Wong, J.L. Andres, M. Head-Gordon, E.S. Replogle, J.A. Pople, GAUSSIAN 98, Gaussian, Inc., Pittsburgh, PA, 1998.

[18] The valence basis sets and effective core potentials for iodine and bromine are taken from: A. Bergner, M. Dolg, W. Küchle, H. Stoll, H.W. Preuβ, Mol. Phys. 80 (1993) 1431. The coefficients for the diffuse and polarization functions are taken from [19].

[19] M.N. Glukhovtsev, A. Pross, M.P. McGrath, L. Radom, J. Chem. Phys. 103 (1995) 1878.

[20] In creating sets of multiple *d* functions from a single optimized function, the normal procedure is to use exponents that are mulitiples $n\alpha_d$ and fractions α_d/n of the single optimized exponent (α_d). When $n=2$ and 4 is used for the splitting into two and three *d* functions, respectively, it is referred to as a geometrical splitting. However, the non-geometrical splittings of $n=3$ (3*d*) in third-row elements, and of $n=1.5$ (2*d*) and $n=2$ (3*d*) in fourth-row elements have been found to be more suitable [19].

[21] Strictly speaking, this is the scaling factor for ZPVEs calculated at the MP2(fc)/6-31G(*d*) level (as opposed to MP2/6-31+G(*d*)), as recommended in: A.P. Scott, L. Radom, J. Phys. Chem. 100 (1996) 16502. However, the ZPVE scaling factors for HF/6-31G(*d*) and HF/6-31+G(*d*) are 0.9135 and 0.9153, respectively, and we assume that the scaling factors for the ZPVEs calculated at MP2(fc) are likely to be equally similar. In Gn methods, it is common practice to use scaling factors optimized for frequencies in the calculation of ZPVEs, with the shortcomings in this approach being absorbed in the higher-level correction (HLC). We use ZPVE scaling factors instead in the present work since the reaction energies and barriers are independent of the HLC.

[22] At the HF/6-31+G(*d*) level, the investigated reactions are in most cases predicted to proceed by way of a double-well potential whereas the MP2(fc)/6-31+G(*d*) level predicts a single well.

[23] E.P. Hunter, S.G. Lias, NIST Standard Reference Database Number 69, November 1998, W.G. Mallard, P.J. Linstrom, (Eds.), National Institute of Standards and Technology, Gaithersburg, MD, 1998 (http://webbook.nist.gov).

[24] T. Ziegler, in Computational Thermochemistry, K.K. Irikura, D.J. Frurip (Eds), ACS Symposium Series, Washington, DC, 1998, p. 369; W. Kutzelnigg, Angew. Chem. Int. Ed. Engl. 23 (1984) 272.

[25] S. Shaik, A. Shurki, Angew. Chem. Int. Ed. Engl. 38 (1999) 587.

[26] J. Emsley, D. Hall, The Chemistry of Phosphorus, Harper and Row, London, 1976, p. 41.

[27] The term “stereospecific” is used to denote a process that is “mechanistically constrained to proceed in a stereochemically defined manner”, as suggested by L.N. Mander, in , Stereochemistry of Organic Compounds, E.L. Eliel, S.H. Wilen (Eds.), Wiley, New York, 1994.

[28] K. Mislow, Accounts Chem. Res. 3 (1970) 321.

[29] R.S. Berry, J. Chem. Phys. 32 (1960) 933.

[30] I. Ugi, D. Marquarding, H. Klusacek, P. Gillespie, Acc. Chem. Res. 4 (1971) 288; P. Gillespie, P. Hoffman, H. Klusacek, D. Marquarding, S. Pfohl, F. Ramirez, E.A. Tsolis, I. Ugi, Angew. Chem. Int. Ed. Engl. 10 (1971) 687.

[31] P. Wang, D.K. Agrafiotis, A. Streitwieser, P.v.R. Schleyer, J. Chem. Soc. Chem. Commun. (1990) 201.